Cation-cation contact pairing in water: Guanidinium

Orion Shih, Alice H. England, Gregory C. Dallinger, Jacob W. Smith, Kaitlin C. Duffey, Ronald C. Cohen, David Prendergast, and Richard J. Saykally

Citation: The Journal of Chemical Physics **139**, 035104 (2013); doi: 10.1063/1.4813281
View online: http://dx.doi.org/10.1063/1.4813281
View Table of Contents: http://scitation.aip.org/content/aip/journal/jcp/139/3?ver=pdfcov
Published by the AIP Publishing

Cation-cation contact pairing in water: Guanidinium

Orion Shih,[1] Alice H. England,[1,2,a)] Gregory C. Dallinger,[1,b)] Jacob W. Smith,[1]
Kaitlin C. Duffey,[1] Ronald C. Cohen,[1] David Prendergast,[3,c)] and Richard J. Saykally[1,2,c)]
[1]*Department of Chemistry, University of California, Berkeley, California 94720, USA*
[2]*Chemical Sciences Division, Lawrence Berkeley National Laboratory, Berkeley, California 94720, USA*
[3]*Molecular Foundry, Lawrence Berkeley National Laboratory, Berkeley, California 94720, USA*

(Received 18 April 2013; accepted 13 June 2013; published online 19 July 2013)

The formation of like-charge guanidinium-guanidinium contact ion pairs in water is evidenced and characterized by X-ray absorption spectroscopy and first-principles spectral simulations based on molecular dynamics sampling. Observed concentration-induced nitrogen K-edge resonance shifts result from π^* state mixing and the release of water molecules from each first solvation sphere as two solvated guanidinium ions associate into a stacked pair configuration. Possible biological implications of this counterintuitive cation-cation pairing are discussed. © *2013 AIP Publishing LLC*. [http://dx.doi.org/10.1063/1.4813281]

I. INTRODUCTION

The discovery of selective interactions between ions and proteins originates from Hofmeister's studies with chicken egg lysozyme, viz., the amount of salt needed to "salt out" the protein depends directly on the ion identities.[1] Such ion-specific effects influence important biological phenomena, such as concentration gradients across membranes, and protein folding and unfolding.[2] In fact, some 40 different phenomena that obey a very similar ordering of both cations and anions with respect to the strength of their effects on the process have been identified.[3] Collins has argued that the tendency of an ion to form contact (inner shell) pairs with the charged carboxylate and amino groups of proteins is directly related to protein "Hofmeister Effects", and more generally, he proposes a "Law of Matching Water Affinities" which governs the tendency of a cation and anion to form a contact pair, viz., if their hydration energies match.[4,5]

Guanidinium ($C(NH_2)_3^+$, Gdm^+) salts are widely used for denaturing protein in solutions.[6] Studies have shown that Gdm^+ promotes protein unfolding by interacting strongly with neutral (both hydrophobic and polar) as well as negatively charged groups.[7] Recently, like-charge ion pairing of Gdm^+, a counterintuitive analogue of ion-specific effects, has received considerable attention. Various computational methods, including *ab initio*,[8,9] Monte Carlo,[10] molecular dynamics (MD) simulations,[9,11,12] and quantum chemical calculations[13,14] have all indicated the existence of contact ion pairing between Gdm^+ ions in water. However, the direct experimental detection of this ion pairing remains elusive: neutron diffraction with isotopic substitution (NDIS) experiments and MD simulations by Mason *et al.* indicated significant ion pairing for the Gdm^+ ions in a stacked geometry,[11] but subsequent investigation using broadband dielectric relaxation spectroscopy revealed only weak pairing for $Gdm_2CO_{3(aq)}$ solutions and no signs of ion-pairing with $GdmCl_{(aq).}$[15] Recently, the measurement of electrophoretic mobilities of oligoarginines indicated an affinity of Gdm^+ for the very similar charged arginine side chains,[16] indirectly implying that the like-charged Gdm^+ pair itself may be stable in water.

In this study, we investigate the electronic structure of GdmCl solutions using X-ray absorption spectroscopy (XAS) of liquid microjets.[17] Since the unoccupied orbitals probed in the experiment extend beyond the Gdm^+ ion itself, the XAS spectrum is generally sensitive to the changes in the local solvation environment, including potential effects of ion-pairing. Similar experiments conducted for NaCl solutions by Aziz *et al.* using a liquid cell produced XAS spectra at the Na K-edge for NaCl solutions as a function of concentration and revealed spectral fingerprints of Na^+–Cl^-contact ion pairs.[18] Later studies by Uejio *et al.* evidenced selective interactions of alkali cations with carboxylate groups at the carbon K-edge.[19] Since the chemical information that can be extracted from such experimental data alone is limited, here we interpret our experimental nitrogen K-edge spectra with a combination of molecular dynamics simulations and a first principles' density functional theory method.[20]

II. METHODS

A. Samples

Guanidine hydrochloride with a purity >99% was purchased from Sigma-Aldrich and used without further purification. 0.5M, 1M, 3M, and 6M (solubility limit) solutions were prepared with Millipore water, which has a resistivity of 18 MΩ/cm.

B. Experimental details

Nitrogen K-edge total electron yield spectra were measured at Beamline 8.0.1 at the Advanced Light Source at

a)Present address: Department of Chemistry, Portland State University, Portland, Oregon 97207, USA.
b)Present address: Department of Chemistry, Wabash College, Crawfordsville, Indiana 47933, USA.
c)Author to whom correspondence should be addressed. Electronic mail: saykally@berkeley.edu

the Lawrence Berkeley National Laboratory. The undulator at Beamline 8 generates intense beam with a maximum flux of 10^{11} photons/s and a resolving power of 4000 E/ΔE, which is focused (~50 μm spot size) onto a liquid jet. The jet itself is produced using a syringe pump (Teledyne-ISCO) to pressurize the liquid behind a fused silica cylindrical nozzle (30 μm ID × 375 μm OD). Soft x-rays intersect the liquid just as it leaves from the tip and total electron yield (TEY) is collected on a positively biased (2.1 kV) copper electrode, yielding room temperature absorption spectra of the bulk liquid.[21,22] The jet subsequently enters a skimmer and condenses on a cryogenic trap. With the turbo pump (Turbotronik NT-20) and one more liquid nitrogen trap placed besides the jet, the main chamber pressure is maintained at ~1.5×10^{-4} torr. Spectra are normalized to the signal from a high transmission gold grid located 2 m upstream from the chamber. The x-ray energy was calibrated to the energy of $1s \rightarrow \pi^*$ resonance of residual nitrogen gas present in the off-jet scan. This vapor signal was then subtracted from the normalized on-jet scan as background subtraction. A more detailed description of the experimental system has been published previously.[17]

C. Calculations

X-ray induced core level excitations are very fast compared to nuclear motion, so the experimental spectra essentially probe molecules in frozen structural configurations, thermodynamically sampled from the vibrational degrees of freedom and solvent structure. To accurately simulate the experimental spectra, transition energies and intensities from multiple molecular dynamics snapshots need to be calculated and averaged.[23,24] AMBER 11 (Ref. 37) was used to perform classical MD simulations of GdmCl solutions, starting with a neutral periodic cubic system containing 10 GdmCl in ionic form and 272 TIP3P water molecules, equivalent to a 1.8M GdmCl solution. The simulations employed the default ff99SB force field with atomic partial charges assigned symmetrically (C 0.64, N −0.80, H 0.46), the non-bonded parameters from OPLS[25,26] were adopted for Gdm^+. After initial energy minimization, the system was heated to 300 K and then equilibrated for 100 ps to a final density under constant pressure condition. A constant volume simulation was then run for 40 ns, with the molecular configuration collected every 1 ps. Since the nitrate anion is the simplest ion that is geometrically analogous to Gdm^+, similar classical MD calculations of $NaNO_3$ with the same concentrations and the same ff99SB force field have been carried out for comparison. The whole MD trajectory was used for radial and spatial distribution analysis but employing randomly chosen snapshots from the trajectory as the input files for XAS calculation will not yield specific information for certain geometrical configuration. Therefore, we set a different periodic box that contains only two GdmCl and 272 TIP3P water molecules, with the same simulation procedure but the snapshots were picked under the carbon-carbon distance constraints: 3.7–3.9 Å for the stacked Gdm^+ pair, 10.0–10.5 Å for the free Gdm^+ pair, and the nitrogen-chloride distance was constrained to 3.2–3.4 Å for two nitrogen atoms in Gdm^+ ion for the $Gdm^+ - Cl^-$ pair. The distances were determined based on the spatial distribution function calculated from the whole, unconstrained trajectory.

Using atomic positions from the snapshots, X-ray absorption spectra were calculated with the XCH density functional theory approach. PWSCF, a part of the Quantum-ESPRESSO package, is used to calculate the electronic structure.[27] We use the Perdew-Burke-Ernzerhof (PBE) form of the generalized gradient approximation to the exchange-correlation potential.[28] A plane wave basis set with periodic boundary conditions was employed to accurately model both localized and delocalized states. The lowest energy core-hole excited state is modeled by inclusion of the eXcited electron and Core Hole (XCH) through the use of a suitably modified pseudopotential. The resulting self-consistent field was used to generate higher excited states non-self consistently. Transition amplitudes for the calculated spectra were calculated within the single particle and dipole approximations. All calculated transitions are numerically broadened by Gaussian convolution of 0.2 eV full width at half maximum. The energy axis is aligned using an atomic alignment scheme introduced previously,[29] designed for comparison between chemically different systems with differing periodic boundary conditions. Only the computed spectrum of isolated nitrogen was aligned to the experimental gas-phase data and all other simulated spectra were aligned relative to that.

III. RESULTS AND DISCUSSION

Figure 1 shows nitrogen K-edge core level spectra of GdmCl at concentrations ranging from 0.5 to 6.0M; spectra are normalized to the peak heights of the first resonance at 401.9 eV for clearer viewing of the electronic structure change at higher photon energy. The overall spectral shape is characterized by two resonances at 401.9 and 404.7 eV, denoted A and B, followed by a broader feature C centered near 410 eV. As the concentration increases, peak B shifts to lower energy with higher intensity. Peak C is too broad to

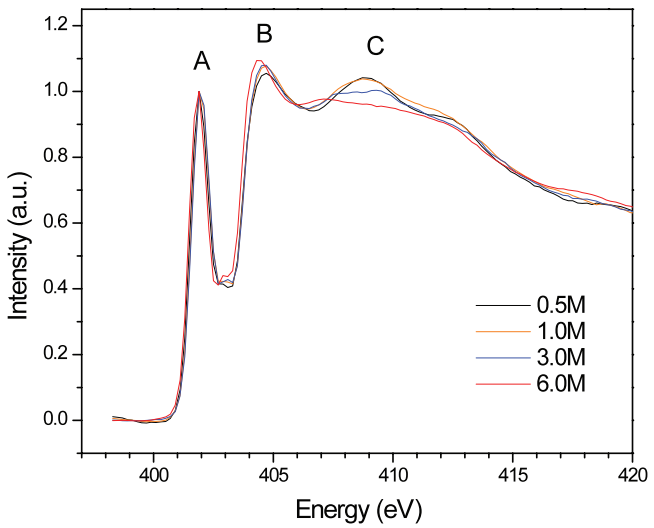

FIG. 1. Measured nitrogen K-absorption edge spectra of aqueous guanidinium chloride solutions for various concentrations. A, B, and C mark the major groups of core level resonances.

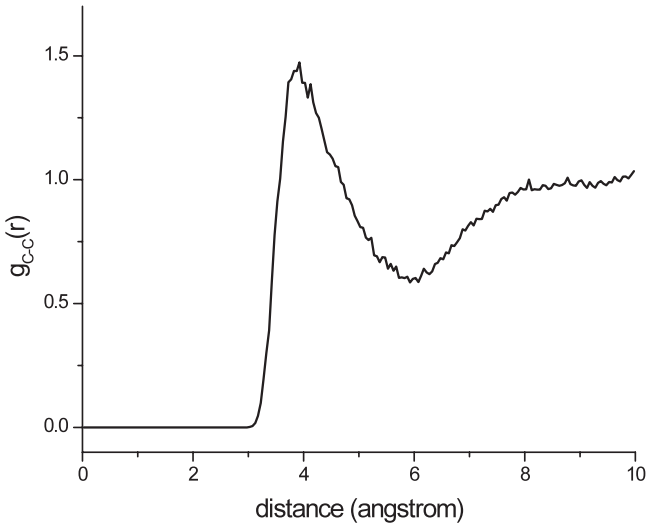

FIG. 2. The carbon-carbon radial distribution function calculated from classical MD simulations of 1.8M GdmCl solution. The broad peak at 3.9 Å demonstrates the formation of contact cation pairs. Details are presented in Sec. II.

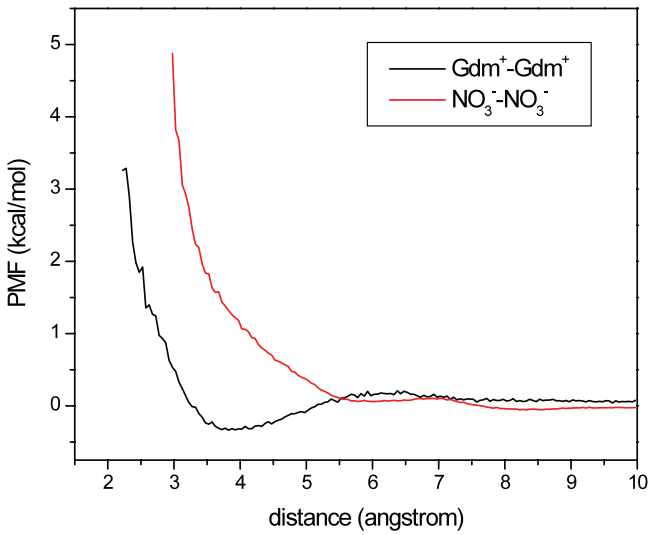

FIG. 4. Potential of mean force for guanidinium ion pairs (black), compared with that for the structurally similar, but independently solvated nitrate ion pairs (red) in water along the C—C(N—N) distance coordinate.

ascertain exactly how the spectral shape varies with concentration; therefore, the analysis will focus on peaks A and B.

To interpret the measured NEXAFS spectra, we perform calculations with the XCH procedure described above. The Gdm^+ carbon-carbon pair correlation function calculated from the MD trajectory is shown in Figure 2; the peak at 3.9 Å indicates a significant tendency for the Gdm^+ ions to form self-associated contact ion pairs (CIP), i.e., Gdm_2^{2+}, since 3.9 Å is larger than the van der Waals contact distance but not large enough for placing one water between the ions. The spatial distribution functions shown in Figure 3 further indicate stacking of pairs of Gdm^+ ions in solution. There is a clear trend for water to accept hydrogen bonds from the hydrogen atoms on Gdm^+. The preferential orientations for water permit simultaneous interaction with hydrogens from two different amine groups while the counter ions (Cl^-) are in competition for the same acceptor sites. There is no recognizable hydration shell around the Gdm^+ ion, and its hydrophobic "face" introduces large voids above and below the molecular plane if it does not bind with another Gdm^+. This observation is consistent with previous MD results.[11]

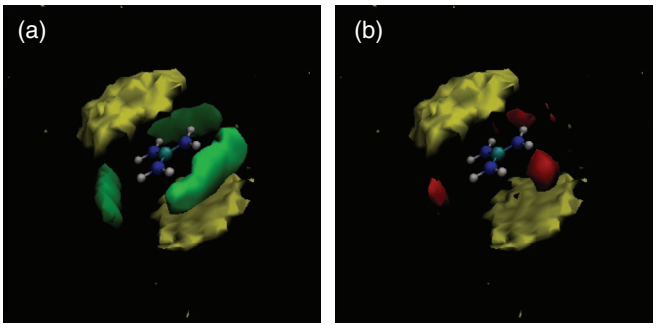

FIG. 3. (a) Calculated spatial distribution function for a 1.8M GdmCl solution showing carbon (yellow, 0.002 atoms $Å^{-3}$) and water (green, 0.025 atoms $Å^{-3}$) density maps around the Gdm^+ ion, demonstrating cation-cation stacked pairing and the preferential binding sites of water. (b) Same spatial distribution function showing carbon (yellow, 0.002 atoms $Å^{-3}$) and chloride (red, 0.002 atoms $Å^{-3}$) distribution.

To evaluate the stability of this counterintuitive cation-cation pairing, the classical potential of mean force (PMF) was calculated using

$$W(r) = -k_B T \, ln \, g(r), \tag{1}$$

where k_B is the Boltzmann constant, T is the temperature, and $g(r)$ is the radial distribution function obtained from the MD calculations. As shown in Figure 4, the computed PMF for two Gdm^+ ions has a well-defined CIP minimum at 3.9 Å and a barrier of 0.53 kcal/mol towards the free pair region where r > 8.0 Å. In contrast, the PMF for the geometrically similar nitrate/nitrate ion pair calculated by the same technique for the same concentration of sodium nitrate solution exhibits the conventional electrostatic repulsive potential, with no attractive behavior evident at short distance.

It is interesting that our potential well is much shallower compared with the PMF previously calculated from Monte Carlo simulations;[10] the CIP is stabilized by 6.73 kcal/mol for the TIP3P water model with a dissociation barrier of 6.26 kcal/mol. There are several differences between the two studies. First, the MC simulations were performed on a single Gdm pair without any counter ions, while in our calculation a realistic solution of 1.8M GdmCl was modeled. Therefore, in the MC study, the Gdm^+ pair is stabilized purely by the strong in-plane hydrogen bond network without the competition of chlorides. Second, Maigret *et al.*[10] constrained the two Gdm^+ ions to remain in parallel planes and kept the ions rigid, whereas we allow free motion, constrained only by molecular configuration and the thermal conditions. The unrealistically rigid structure along with the staggered configuration used in Ref. 7 minimizes the electrostatic and steric repulsion and also optimizes the quadrupole-quadrupole interactions, resulting in a deeper well compared to our PMF, presented in Figure 4. The previous MD studies[9,11] reported a similar carbon-carbon radial distribution function, and would therefore yield a similar PMF curve like ours even though they use both a different water model and force field parameters;

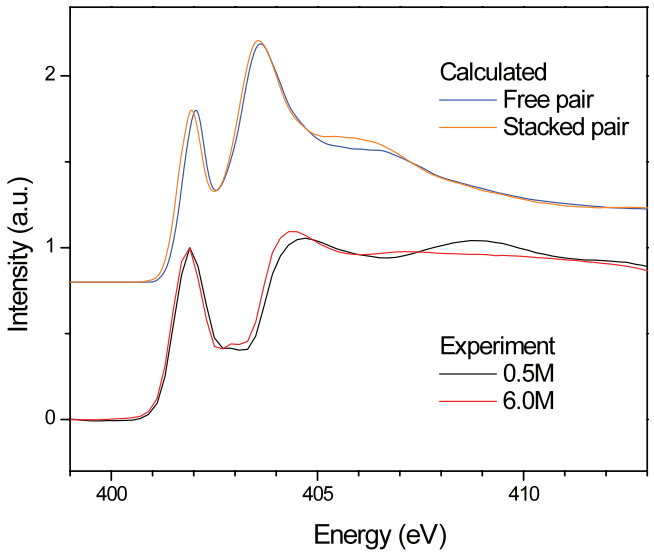

FIG. 5. Upper: Calculated nitrogen K-edge spectra for free and stacked Gdm^+ pairs. Each spectrum represents the average of 100 individual spectra. Lower: experimental nitrogen K-edge spectra for the lowest and highest concentrations: 0.5M and 6.0M solutions. All spectra have been normalized with the peak heights of the first resonance. Compared to the experimental spectra, the calculated spectra exhibit a smaller spacing between the first resonance group at 401.9 eV and the second broader peak because of the well-known tendency of DFT to underestimate the water bandgap. The higher energy resonances are primarily water-rich states, hence the simulated transition energy is affected by this artifact.

hence, the different dissociation barriers are a result of the fundamental differences between the Monte Carlo and MD simulations.

To illustrate the spectral signatures of this cation-cation pairing, Figure 5 presents calculated NEXAFS spectra of stacked and free pairs of Gdm^+ ions in water, along with the experiment results. The simulated spectra show similar resonance peaks, A, B, and C, as observed in the experiment, but with smaller spacing between the features. This results from the underestimation of electronic band width by our semi-local PBE calculations. A typical simulated spectrum with the corresponding isosurfaces is shown in Figure 6, wherein the excited nitrogen is marked by an asterisk. As seen from the isosurface, peak A is composed of two peaks: A1 at 401.91 eV and A2 at 402.04 eV. A1 (LUMO) represents a transition from the 1*s* orbital to a localized $s\sigma^*$ state with mixture of π character on other atoms, whereas A2 (LUMO+1) comprises a transition to a pure π^* state, with 3–7 times higher oscillator strength than that of A1, depending on the molecular configurations. Interestingly, our ground state PBE calculations indicate that the LUMO of Gdm^+ has pure π^* character and a LUMO+1 state with $s\sigma^*(NH_2)$ character, which is the opposite ordering observed in the core-excited state. Figure 7 further demonstrates this orbital reversal by displaying the isosurfaces of ground state and core-excited bare Gdm^+ (without waters). When an electron is excited from a nitrogen core level, the effective nuclear charge increases and that nitrogen appears to the valence electrons as an oxygen atom, lowering the orbital energies. Because σ orbitals penetrate closer to the nucleus, their energy will decrease more than that of the π state, leading to the orbital reversal.

This core excitation-induced orbital reversal is also found in similar nitrogen-containing delocalized systems, such as aniline ($C_6H_5NH_2$), for which *ab initio* calculations revealed $\sigma^*(NH_2)$ character for the aniline LUMO.[30,31] With their higher experimental resolution, Duflot *et al.* suggested a 3*s* Rydberg orbital with $\sigma^*(NH_2)$ character.[32] There have been some debates on assignments of the LUMO+1: the EICVOM model[2,6–31] revealed π^* character, whereas others showed a different level mixing of 3*p* Rydberg orbital, $\sigma^*(NH_2)$ and π^*.[30,32,33] However, if the amine group is replaced by a nitro group ($-NO_2$) the N 1*s* spectrum would be dominated by the strong N1$s \rightarrow \pi^*_{NO}$ transition (LUMO) and there is no orbital reversal, due to the unsaturated character of the nitro group.

In addressing the role of water in the unoccupied molecular-orbital electronic structure, it is useful to examine the projected density of states (DOS) of water and Gdm^+

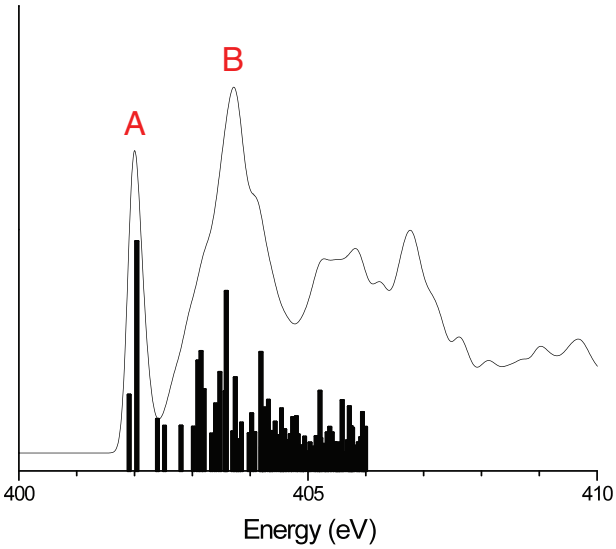

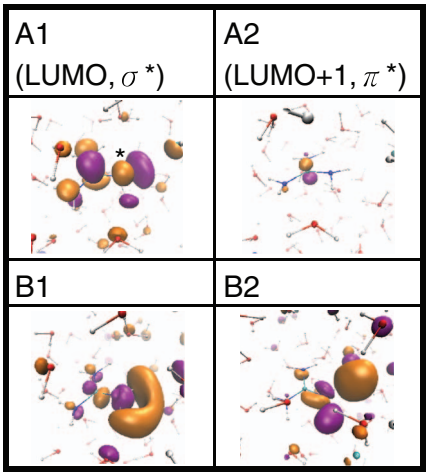

FIG. 6. Single snapshot spectra with stick spectra and associated states (15% isosurface) for free Gdm^+ pair. Peak A comprises two transitions, A1 (1*s* $\rightarrow$ $s\sigma^*(NH_2)$, 401.91 eV) and A2 (1*s* $\rightarrow$ π^*, 402.04 eV). Lower panel shows the strongest transitions B1 (403.10 eV) and B2 (403.59 eV) in Peak B group.

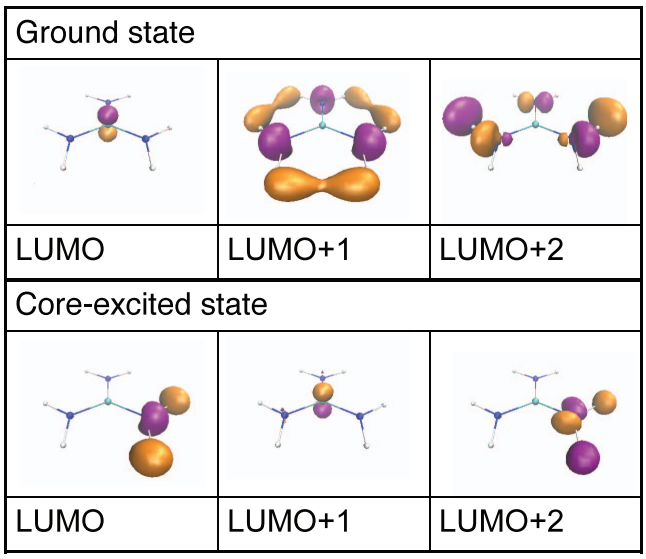

FIG. 7. Comparison of the unoccupied states for ground state and core-excited Gdm^+ ion.

(Figure 8). The first peak of the H_2O DOS matches the energy of resonance A1, while the first peak of Gdm^+ DOS matches that of resonance A2. A2 is also the state that has the highest Gdm^+ DOS and the only state with a Gdm^+ DOS higher than that of H_2O, making it the strongest transition, as observed in our spectra. Peak B reveals a large number of resonances from the hybridization with surrounding water molecules. Figure 6 displays the isosurfaces of the two strongest resonances in the peak B group—B1 at 403.10 eV and B2 at 403.59 eV. B1 represents the transition from the 1*s* orbital to a localized $s\sigma^*$ state mixing with π^* character on other atoms. It is similar to A1 but with higher contributions from H_2O DOS, i.e., a more diffuse state. The B2 feature originates from the LUMO+2 state of the bare Gdm^+ ($p\sigma^*(NH_2)$, see Figure 7), which couples to surrounding water molecules.

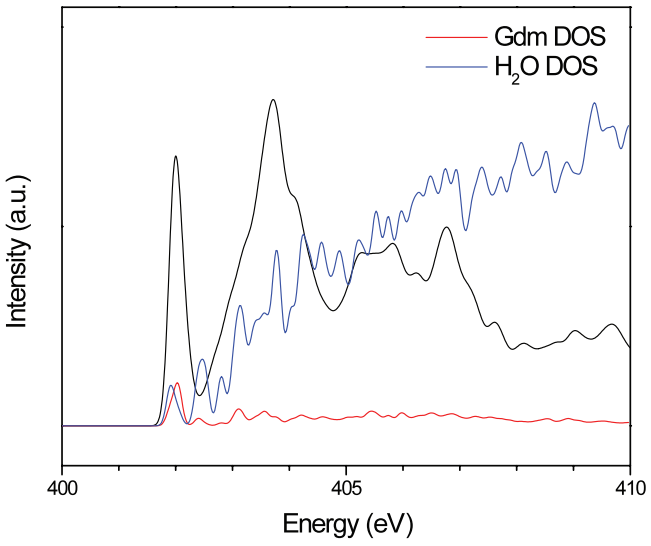

FIG. 8. Sample snapshot spectrum with corresponding projected Gdm^+ and water density of states.

For both peaks A and B, the trend of spectral redshift from free to stacked pairs, matches with the experimental observation of a redshift when moving from lower to higher concentrations. The redshift in peak A can be explained by state mixing between the components of the Gdm^+ pair: as the two Gdm^+ ions approach closely, the two π systems interact and create a more delocalized charge distribution, thus stabilizing the π^* state, which is the major component of peak A. For peak B, the σ system interacts more weakly with the other Gdm^+ ion, so the observed redshift must be related to the surrounding solvation environment. Figure 8 demonstrates that peak B is mainly composed of water-rich states, so that it will be sensitive to water-water interactions. When two solvated Gdm^+ ions associate, they release water molecules from their own solvation shells, and the water hydrogen-bond network becomes extended, again stabilizing the final states. This results in the redshift of peak B in the calculated spectra, moving from free to stacked pairs. In our experiments, the same trend of spectral redshift of peaks A and B is observed when moving from low to high concentrations; therefore, we reach the conclusion that as concentration increases, there is a higher probability for contact ion pairing between Gdm^+ ions. If no contact ion pairs form, the electronic structure of the Gdm^+ ions would not be expected to vary so much with concentration.

As evident in the density map in Figure 3(b), chloride ion has the possibility of associating with Gdm^+ ions. To explore the spectral effects of the formation of a Gdm^+-chloride contact pair, its XAS spectra calculated under the same conditions as in Figure 5 are shown in Figure 9, compared with the simulated spectra of both guanidinium free pair and stacked pair (same spectra shown in Figure 5). All spectra are normalized to the peak heights of the first resonance (A). The Gdm^+-chloride pair exhibits the same essential spectral shapes, with

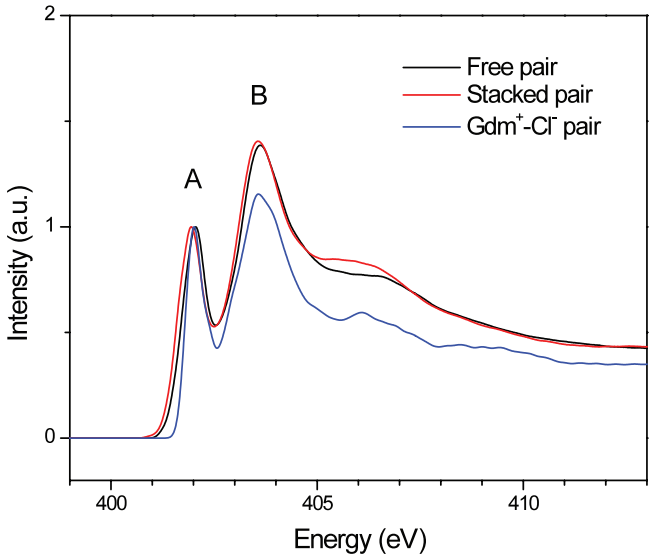

FIG. 9. Calculated nitrogen K-edge spectra for free Gdm^+ pairs, stacked Gdm^+ pairs, and Gdm^+–Cl^- pairs. The carbon-carbon distance was constrained to 10.0–10.5 Å for the free pairs and 3.7–3.9Å for the stacked pairs. The nitrogen-chloride distance was constrained to 3.2–3.4 Å for two nitrogen atoms in Gdm^+ ion for the Gdm^+–Cl^- pair. All spectra have been normalized with the peak heights of the first resonance A.

resonance A situated at the same energy as that of the free guanidinium pair. This is expected because resonance A is sensitive only to the π^* interaction, and the encounter with a chloride ion at the side of the guanidinium ion does not affect the π system. The most noticeable difference is the intensity of resonance B, which drops 17% relative to that of the free pair. Since resonance B is sensitive to the solvation environment; when chloride ion enters the first solvation shell of guanidinium, it disrupts the water hydrogen-bond network and decreases the spatial overlap with the water states, which produces the lower signal intensity. However, this predicted drop in intensity of resonance B is not observed in our experiments as the salt concentration increases, implying insignificant Gdm^+-chloride pair formation, at least, not comparable to the Gdm^+-Gdm^+ ion pair formation. However, we do note that control experiments, wherein NaCl is systematically added to the guanidinium chloride solutions, were not preformed here, and the above conclusion rests primarily on the comparison between our detailed calculations and experiment that is presented.

The association of two weakly hydrated (chaotropic) Gdm^+ ions represents a remarkable ion-specific effect. Since Gdm^+ corresponds to the side chain of arginine, which is protonated at biological pH, a similar pairing between Gdm^+ ion and arginine side chains of proteins could exist. It is believed that there are two principal mechanisms for ion-induced protein unfolding: direct interaction of the ion with some parts of the protein or modification of the solvating water structure. The direct interaction model has been indicated as having a primary relevance in protein destabilization by Gdm^+ salts[15,34] but the temperature-excursion IR study by Scott *et al.* also showed a substantial restructuring of the water H-bond network upon addition of GdmCl.[35] Our technique probes both the direct interaction and the change on the solvation environment, but cannot easily separate the relative contribution of the two mechanisms.

To further support the interpretation of the observed spectral shifts, we examine calculated spectra of GdmCl in crystalline form. The crystal structure data were taken from Haas *et al.*[36] GdmCl crystallizes in the orthorhombic system with space group *Pbca*. The crystal structure consists of chloride ions coordinated by three different Gdm^+ ions, two of which are coplanar. The third Gdm^+ ion is nearly perpendicular to this plane. Figure 10 depicts the atomic arrangement around Gdm^+ in the crystal: Each Gdm^+ coordinates to three chloride ions, with two of these chloride ions associating onto another Gdm^+ which is coplanar with the original one, and the same unit is repeated, forming a chain-like structure. As shown in Figure 10, the three lower Gdm^+ ions are in the same plane and the planar Gdm^+—Cl^-—Gdm^+—Cl^- structure is repeated along x-axis. The top chloride ion coordinated to N1 and N2 is different, binding with two other Gdm^+ ions, neither of which is in the same plane displayed in Figure 10. From symmetry considerations, if the crystal were perfect, N1 and N2 would be equivalent, but there is actually a small variation in the chloride-nitrogen distances. The average N1-(top chloride) distance is 3.27 Å, while 3.36 Å is found for N2-(top chloride) distance. Therefore, there are three different types of nitrogen atoms in the crystal, N1, N2, and N3. The corresponding calculated spectra are shown in Figure 11, along with the spectra of bare Gdm^+ and solvated free Gdm^+ pair taken from Figure 5. The overall spectral shape of N1 and N2 spectra are similar, but with a shift on the first peak resulting from the same $1s \rightarrow$ LUMO ($s\sigma^*(NH_2)$, π^* mixed state) and $1s \rightarrow$ LUMO+1 (π^*) resonances described earlier. Since N1 has a smaller distance to the N2-shared chloride (3.27 Å) compared to that of N2 (3.36 Å), N1 experiences stronger interaction with chloride. This preferential interaction stabilizes the bonding orbitals and shifts the anti-bonding orbitals to higher energy, resulting in the blue shift of the first peak in the N1 spectrum, compared with that of N2. The N3 spectrum exhibits unique features: an even lower energy peak A and strong resonances at 403.4 eV, which is roughly the same energy as peak B in the spectrum of the solvated free Gdm^+ pair. Being a nitrogen coordinated by two chlorides that associate with other Gdm^+ ions in the same plane, the LUMO and

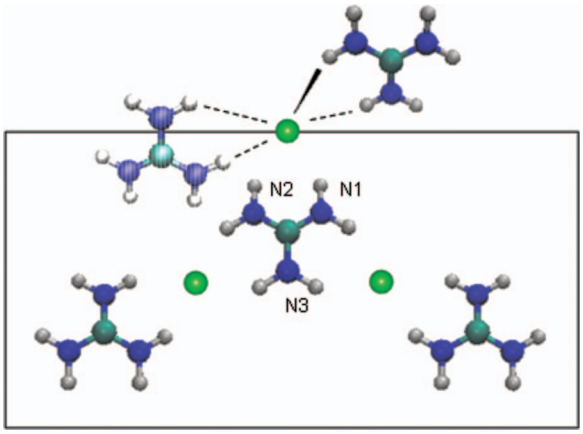

FIG. 10. Arrangement of the guanidinium and chloride ions in the crystal. The three lower guanidinium ions and three chloride ions (green) are in the same plane, the top chloride coordinates with the top two guanidinium ions, which are not in the same plane.

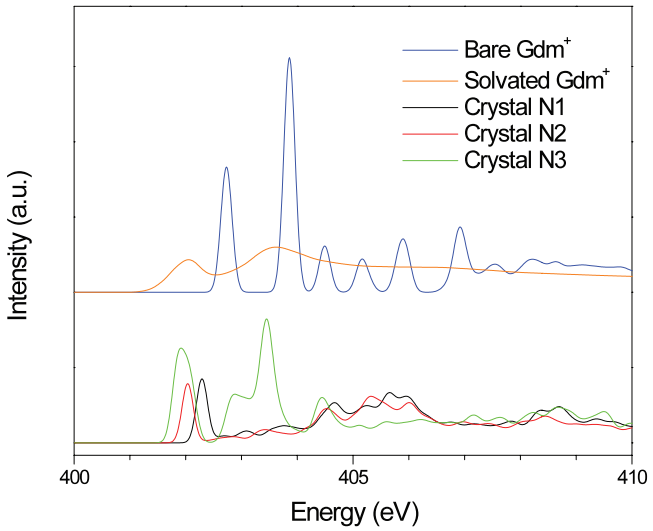

FIG. 11. Calculated spectra due to individual nitrogen atom excitation in crystalline guanidinium chloride, compared with calculated spectra of an isolated guanidinium ion and a solvated guanidinium free pair. All spectra are processed with energy alignment but without intensity normalization.

LUMO+1 of N3 are delocalized states extending through the chain-like structure shown in the bottom of Figure 10. This delocalization shifts the resonance to a lower energy, as explained above. The strong resonance at 403.4 eV originates from the $1s \rightarrow$ LUMO+2 state of bare Gdm^+ ($p\sigma^*(NH_2)$) also extends throughout the Gdm^+–Cl^- chain, lowering the energy. In comparison, the spectrum of bare Gdm^+ exhibits no delocalization, and peaks A and B are then blue shifted compared to the solvated free pair.

IV. CONCLUSIONS

We have measured the nitrogen K-edge NEXAFS spectra of aqueous GdmCl solutions at various concentrations and observed spectral fingerprints with sensitivity to concentration that match with first-principles electronic structure calculations which sample classical molecular dynamics trajectories at 300 K. Theoretical interpretation indicates that the first observed spectral resonance, at 401.9 eV, is dominated by N $1s \rightarrow \pi^*$ transitions and is red-shifted due to intermolecular π^* system mixing at high concentrations. The second resonance, at 404.7 eV, reflects interactions with the water hydrogen bonding network, and reveals a greater chance to form like-charged guanidinium-guanidinium pairs with increasing concentration. The present results demonstrate the sensitivity of our experiments and analysis using the XCH electronic structure approach for probing such weak cation-cation interactions. Overcoming the repulsive Coulomb forces between two cations to form a stable ion pair in water is an interesting manifestation of ion-specific effects and provides a possible mechanism for protein unfolding induced by guanidinium salts. Other biological interactions could possibly involve similar like-charge ion pairing, e.g., nucleotide/nucleoside-protein interactions.

ACKNOWLEDGMENTS

This work was supported by the Director, Office of Basic Energy Sciences, Office of Science, U.S. Department of Energy (DOE) under Contract No. DE-AC02-05CH11231, through the LBNL Chemical Sciences Division and as part of a user project at the Molecular Foundry. Computational resources were provided by the National Energy Research Scientific Computing Center and the Molecular Graphics and Computation Facility (College of Chemistry, University of California, Berkeley) under NSF grant CHE-0840505. The authors would also like to thank Wanli Yang and Jonathan Spear for beamline support at the Advanced Light Source.

[1]F. Hofmeister, Arch. Exp. Pathol. Pharmacol. **24**, 247 (1888).
[2]J. M. Berg, J. L. Tymoczko, and L. Stryer, *Biochemistry* (W. H. Freeman, New York, 2002).
[3]K. D. Collins and M. W. Washabaugh, Q. Rev. Biophys. **18**, 323 (1985).
[4]K. D. Collins, Biophys. Chem. **119**, 271 (2006).
[5]K. D. Collins, Methods **34**, 300 (2004).
[6]T. Svedberg, Nature (London) **139**, 1051 (1937).
[7]C. E. Dempsey, T. J. Piggot, and P. E. Mason, Biochemistry **44**, 775 (2005).
[8]K. T. No, K. Y. Nam, and H. A. Scheraga, J. Am. Chem. Soc. **119**, 12917 (1997).
[9]J. Vondrasek, P. E. Mason, J. Heyda, K. D. Collins, and P. Jungwirth, J. Phys. Chem. B **113**, 9041 (2009).
[10]S. Boudon, G. Wipff, and B. Maigret, J. Phys. Chem. **94**, 6056 (1990).
[11]P. E. Mason, G. W. Neilson, J. E. Enderby, M. L. Saboungi, C. E. Dempsey, A. D. MacKerell, Jr., and J. W. Brady, J. Am. Chem. Soc. **126**, 11462 (2004).
[12]J. C. Soetens, C. Millot, C. Chipot, G. Jansen, J. G. Angyan, and B. Maigret, J. Phys. Chem. B **101**, 10910 (1997).
[13]M. Vazdar, J. Vymetal, J. Heyda, J. Vondrasek, and P. Jungwirth, J. Phys. Chem. A **115**, 11193 (2011).
[14]A. K. H. Weiss, T. S. Hofer, B. R. Randolf, and B. M. Rode, Phys. Chem. Chem. Phys. **14**, 7012 (2012).
[15]J. Hunger, S. Niedermayer, R. Buchner, and G. Hefter, J. Phys. Chem. B **114**, 13617 (2010).
[16]A. Kubickova, T. Krizek, P. Coufal, E. Wernersson, J. Heyda, and P. Jungwirth, J. Phys. Chem. Lett. **2**, 1387 (2011).
[17]K. R. Wilson, B. S. Rude, J. Smith, C. D. Cappa, D. T. Co, R. D. Schaller, M. Larsson, T. Catalano, and R. J. Saykally, Rev. Sci. Instrum. **75**, 725 (2004).
[18]E. F. Aziz, A. Zimina, M. Freiwald, S. Eisebitt, and W. Eberhardt, J. Chem. Phys. **124**, 114502 (2006).
[19]J. S. Uejio, C. P. Schwartz, A. M. Duffin, W. S. Drisdell, R. C. Cohen, and R. J. Saykally, Proc. Natl. Acad. Sci. **105**, 6809 (2008).
[20]D. Prendergast and G. Galli, Phys. Rev. Lett. **96**, 215502 (2006).
[21]C. D. Cappa, J. D. Smith, K. R. Wilson, and R. J. Saykally, J. Phys.: Condens. Matter **20**, 205105 (2008).
[22]K. R. Wilson, B. Rude, T. Catalano, R. Schaller, J. G. Tobin, D. T. Co, and R. J. Saykally, J. Phys. Chem. B **105**, 3346 (2001).
[23]C. P. Schwartz, J. S. Uejio, R. J. Saykally, and D. Prendergast, J. Chem. Phys. **130**, 184109 (2009).
[24]J. S. Uejio, C. P. Schwartz, R. J. Saykally, and D. Prendergast, Chem. Phys. Lett. **467**, 195 (2008).
[25]J. Chandrasekhar, D. C. Spellmeyer, and W. L. Jorgensen, J. Am. Chem. Soc. **106**, 903 (1984).
[26]W. L. Jorgensen and J. Tirado-Rives, J. Am. Chem. Soc. **110**, 1657 (1988).
[27]P. Giannozzi, S. Baroni, N. Bonini, M. Calandra, R. Car, C. Cavazzoni, D. Ceresoli, G. L. Chiarotti, M. Cococcioni, I. Dabo, A. Dal Corso, S. de Gironcoli, S. Fabris, G. Fratesi, R. Gebauer, U. Gerstmann, C. Gougoussis, A. Kokalj, M. Lazzeri, L. Martin-Samos, N. Marzari, F. Mauri, R. Mazzarello, S. Paolini, A. Pasquarello, L. Paulatto, C. Sbraccia, S. Scandolo, G. Sclauzero, A. P. Seitsonen, A. Smogunov, P. Umari, and R. M. Wentzcovitch, J. Phys. Condens. Matter **21**, 395502 (2009).
[28]J. P. Perdew, K. Burke, and M. Ernzerhof, Phys. Rev. Lett. **77**, 3865 (1996).
[29]A. H. England, A. M. Duffin, C. P. Schwartz, J. S. Uejio, D. Prendergast, and R. J. Saykally, Chem. Phys. Lett. **514**, 187 (2011).
[30]O. Plashkevych, L. Yang, O. Vahtras, H. Agren, and L. G. M. Pettersson, Chem. Phys. **222**, 125 (1997).
[31]A. C. O. Guerra, G. B. Ferreira, S. P. Machado, and C. C. Turci, Int. J. Quantum Chem. **108**, 2340 (2008).
[32]D. Duflot, J. P. Flament, A. Giuliani, J. Heinesch, M. Grogna, and M. J. Hubin-Franskin, Phys. Rev. A **75**, 052719 (2007).
[33]C. C. Turci, S. G. Urquhart, and A. P. Hitchcock, Can. J. Chem. **74**, 851 (1996).
[34]C. N. Pace, Methods Enzymol. **131**, 266 (1986); P. E. Mason, G. W. Neilson, C. E. Dempsy, A. C. Barnes, and J. M. Cruickshank, Proc. Natl. Acad. Sci. U.S.A. **100**, 4557 (2003); S. N. Timasheff, Biochemistry **31**, 9857 (1992); E. P. O'Brien, R. I. Dima, B. Brooks, and D. Thirumalai, J. Am. Chem. Soc. **129**, 7346 (2007); R. D. Mountain and D. J. Thirumalai, J. Phys. Chem. B **108**, 19711 (2004).
[35]J. N. Scott, N. V. Nucci, and J. M. Vanderkooi, J. Phys. Chem. A **112**, 10939 (2008).
[36]D. J. Haas, D. R. Harris, and H. H. Mills, Acta Crystallogr. **19**, 676 (1965).
[37]D. A. Case, T. A. Darden, T. E. Cheatham, III, C. L. Simmerling, J. Wang, R. E. Duke, R. Luo, R. C. Walker, W. Zhang, K. M. Merz, B. Roberts, B. Wang, S. Hayik, A. Roitberg, G. Seabra, I. Kolossváry, K. F. Wong, F. Paesani, J. Vanicek, J. Liu, X. Wu, S. R. Brozell, T. Steinbrecher, H. Gohlke, Q. Cai, X. Ye, J. Wang, M.-J. Hsieh, G. Cui, D. R. Roe, D. H. Mathews, M. G. Seetin, C. Sagui, V. Babin, T. Luchko, S. Gusarov, A. Kovalenko, and P. A. Kollman, AMBER 11 (University of California, San Francisco, 2010).